Applied Surface Science 347 (2015) 169–177

Contents lists available at ScienceDirect

Applied Surface Science

journal homepage: www.elsevier.com/locate/apsusc

Construction of a multifunctional coating consisting of phospholipids and endothelial progenitor cell-specific peptides on titanium substrates

Huiqing Chen [a], Xiaojing Li [a], Yuancong Zhao [a,*], Jingan Li [a], Jiang Chen [a], Ping Yang [a,*], Manfred F. Maitz [a,b], Nan Huang [a]

[a] Key Lab. of Advanced Technology for Materials of Education Ministry, School of Materials Science and Engineering, Southwest Jiaotong University, Chengdu 610031, PR China
[b] Max Bergmann Center of Biomaterials Dresden, Leibniz of Polymer Research Dresden, 01069 Dresden, Germany

ARTICLE INFO

Article history:
Received 14 November 2014
Received in revised form 3 February 2015
Accepted 4 February 2015
Available online 12 February 2015

Keywords:
Titanium
Phospholipid
Specific peptide
Endothelial progenitor cells
Biomimetic multifunctional coating

ABSTRACT

A phospholipid/peptide polymer (PMMDP) with phosphorylcholine groups, endothelial progenitor cell (EPC)-specific peptides and catechol groups was anchored onto a titanium (Ti) surface to fabricate a biomimetic multifunctional surface. The PMMDP coating was characterized by X-ray photoelectron spectroscopy (XPS), water contact angle measurements and atomic force microscopy (AFM), respectively. The amount of PMMDP coating on the Ti surface was quantified by using the quartz crystal microbalance with dissipation (QCM-D). Interactions between blood components and the coated and bare Ti substrates were evaluated by platelet adhesion and activation assays and fibrinogen denaturation test using platelet rich plasma (PRP). The results revealed that the PMMDP-modified surface inhibited fibrinogen denaturation and reduced platelet adhesion and activation. EPC cell culture on the PMMDP-modified surface showed increased adhesion and proliferation of EPCs when compared to the cells cultured on untreated Ti surface. The inhibition of fibrinogen denaturation and platelet adhesion and support of EPCs attachment and proliferation indicated that this coating might be beneficial for future applications in blood-contacting implants, such as vascular stents.

1. Introduction

Optimal biomaterials should perform their function without causing undue host response or inducing adverse clinical outcomes [1,2]. However, thrombosis and neointimal hyperplasia are the major factors that limit the application of blood-contacting materials for the treatment of blood vessel diseases such as coronary artery disease (CAD) and peripheral vascular disease (PVD) [3,4]. It is well known that the endothelium effectively inhibits both thrombosis and neointimal hyperplasia in vessels after implantation [5,6]. Therefore, it is crucial to the success of cardiovascular implants such as stents, vascular grafts, and heart valves to restore the normal endothelial function by means of rapid re-endothelialization of the injured intima and implant.

In 1997, the discovery of circulating endothelial progenitor cells (EPCs) [7] brought new perspectives for the in vivo/in situ endothelialization of implanted, blood-contacting materials. EPCs are bone marrow-derived cells that circulate at low concentrations in the peripheral blood of adults and possess the ability to proliferate, migrate, and differentiate into functional endothelium, which maintains optimal haemostasis and minimizes the risk of restenosis [8,9]. EPCs are clinically highly significant for the cardiovascular physiology. They participate in endothelial homeostasis and promote the formation of new blood vessels [10]. Till date, the latest strategy for EPC homing on vascular stents has been coating the stents with capture molecules to mimic a natural homing substrate for fishing out EPCs directly from the bloodstream after implantation. Various types of capture molecules, including antibodies [11,12], peptides [13,14], oligosaccharides [15,16], and DNA-aptamers [17], have been utilized to attract EPCs on artificial devices.

EPCs can be classified into "early-EPCs" and "late-EPCs" [18]. "Early-EPCs" share some endothelial and monocytic features [19,20]; they exhibit only a restricted capacity of expansion. In contrast, "late-EPCs", also known as human blood out growth endothelial cells (HBOECs), exhibit cobblestone morphology and long term proliferative potential [21]. Recently, a series of novel peptide

* Corresponding authors. Tel.: +86 28 87634148; fax: +86 28 87600625.
E-mail addresses: zhaoyc7320@163.com (Y. Zhao), yangping8@263.net (P. Yang).

http://dx.doi.org/10.1016/j.apsusc.2015.02.032
0169-4332/

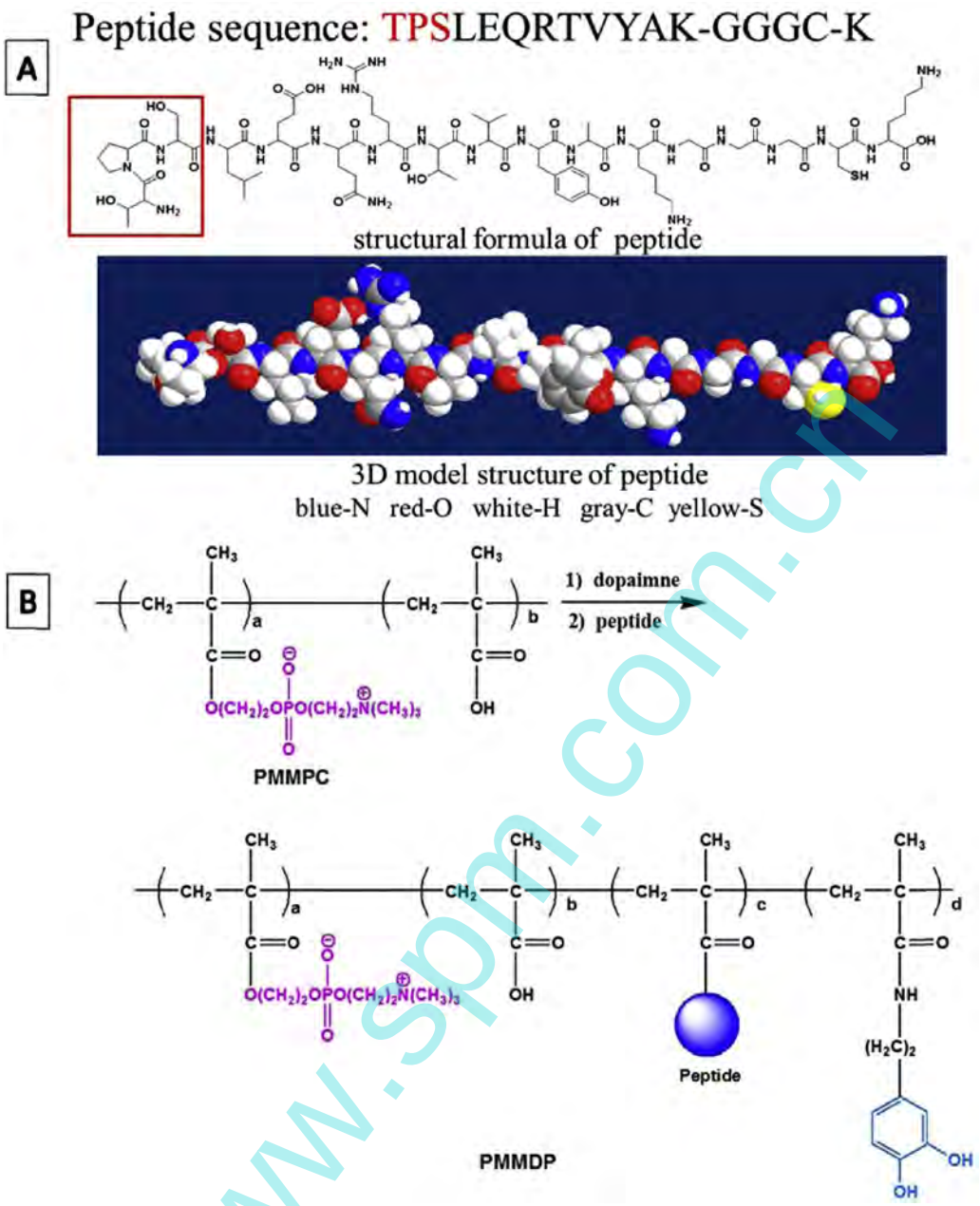

Fig. 1. (A) Structural formula and 3D model of the EPC-peptide aptamer; (B) scheme of PMMDP synthesis.

ligands that selectively binds to late-EPCs has been developed via screening a combinatorial peptide library and phage display technique [13]. Among these peptide ligands, the peptide TPSLEQRTVYAK exhibited the highest affinity and specificity to HBOECs and did not interfere with the endothelial cell (EC) function [4].

Furthermore, the anti-thrombogenic property of a blood-contacting surface is required as long as endothelialization has not been completed. In this study, 2-methacryloyloxyethyl phosphorylcholine (MPC) copolymer was chosen as the constituent for this purpose. MPC polymer and its copolymer have been widely used to construct non-biofouling surfaces for various biomedical applications and to prevent protein adsorption [22]; the MPC co-polymer contains a zwitterionic phospholipid group that is also present in cell membranes, and possesses nonthrombogenic properties and high biocompatibility. At present, there are many reports on surface immobilization of MPC polymers on Ti and its alloy substrates [23]. However, these methods have various limitations for widespread practical use.

To facilitate convenient adhesion of organic compounds to metal substrates, mussel-inspired chemistry has been widely investigated [24]. Mussels can adhere rapidly and permanently to all types of surfaces in aqueous environments. Their adhesive property is based on the catechol group of 3, 4-dihydroxy-l-phenylalanine (DA) found in the mussel foot proteins. Although the exact mechanism of adhesion is not fully understood, it has been widely speculated that the catechol group of DA is responsible for the adhesion [25].

Many studies focus on modifying materials using ligands for the adhesion receptors, such as the RGD peptide, to promote cell adhesion via specific interaction. However, it is a special task to fabricate a surface with anti-adhesive properties to most proteins and cells, except the selectivity for a specific target cell type. Recently, Ji et al.

have developed a zwitterionic poly(carboxybetaine) (PCB) coating functionalized with REDV peptide to improve selectivity of ECs [26].

In this study, we aim to develop a material that provides antifouling properties and promotes endothelialization by recruiting EPCs. For this purpose, we used a modified peptide (Fig. 1A), consisting of an active peptide sequence (TPSLEQRTVYAK) to capture EPCs and a flexible linker sequence (GGGC) to provide structural flexibility. The synthesized poly(2-methacryloyloxyethyl phosphorylcholine-*co*-methacrylic acid) grafted dopamine and peptide (PMMDP), which contain phosphorycholine groups, the EPC-specific peptides and catechol groups, were anchored onto a Ti surface to fabricate a biomimetic surface that resists platelet adhesion and selectively captures EPCs [13,22].

2. Materials and methods

2.1. Materials and reagents

Titanium (Ti) substrates (10 mm × 10 mm) were purchased from Baoji Non-ferrous Metal Co., Ltd. (Baoji, China). The EPCs-specific peptide (PP) was bought from GL Biochem Ltd. (Shanghai, China). Water-soluble 2-methacryloyloxyethyl phosphorylcholine (MPC, 96%) was obtained from the Joy-Nature Technology Institute (China) and used without further purification. Methacrylic acid (MA) and ethanol were bought from KeLong Chemical Co., Ltd. (Chengdu, China); MA was purified by reduced pressure distillation, and ethanol was dried over metal Na and distilled prior use. Dopamine hydrochloride (DA, 99%) and 1-ethyl-3-dimethylaminopropyl carbodiimide (EDC, 98%) were obtained from Sigma–Aldrich (USA). Modified Eagle's medium (a-MEM), and fetal bovine serum (FBS) were obtained from Hyclone (Utah, USA). Cell counting kit-8 (CCK-8) for EC culture and proliferation test were obtained from BD Biosciences (San Jose, CA, USA). All the other reagents were local products and were of analytical grade.

2.2. Synthesis of phospholipid/peptide co-polymer (PMMDP)

The polymer (PMMPC) was synthesized by free-radical copolymerization between MPC and MA [27]. The dopamine-modified PMMPC was named PMMDA. The phospholipid/peptide copolymer (PMMDP) was synthesized by a two-step condensation reaction to graft the dopamine and the peptide to PMMPC. The reaction scheme is presented in Fig. 1B. The two condensation reactions were carried out at room temperature for 6 h under Ar gas to prevent the oxidation of the catechol groups. The molar ratios [dopamine hydrochloride]/[–COOH] and [peptide]/[–COOH] were 0.75 and 0.5, respectively. The products of the two reactions were dialyzed using ultrafiltration membranes (Millipore Co., USA, molecular size cut off: 1.0×10^4), until there was no further release of unreacted dopamine and peptide through the membrane. In addition, the grafted amounts of dopamine and peptide were confirmed by ultraviolet adsorption (UV-2550, Shimadzu, Japan) and the polymers were subsequently frozen and dried for further use.

2.3. Characterization of PMMDP

The infrared absorption spectra of PMMDP were obtained using an FTIR spectrometer (NICOLET 5700, USA) in diffuse reflectance mode. For each of the obtained spectrum, a total of 64 scans were accumulated at 4 cm^{-1} resolution and scanning was conducted in the range of 400–4500 cm^{-1}.

2.4. Surface modification of Ti sheets using PMMDP

The Ti sheets were polished and ultrasonically cleaned thrice using acetone, ethanol, and deionized water, each for 5 min and

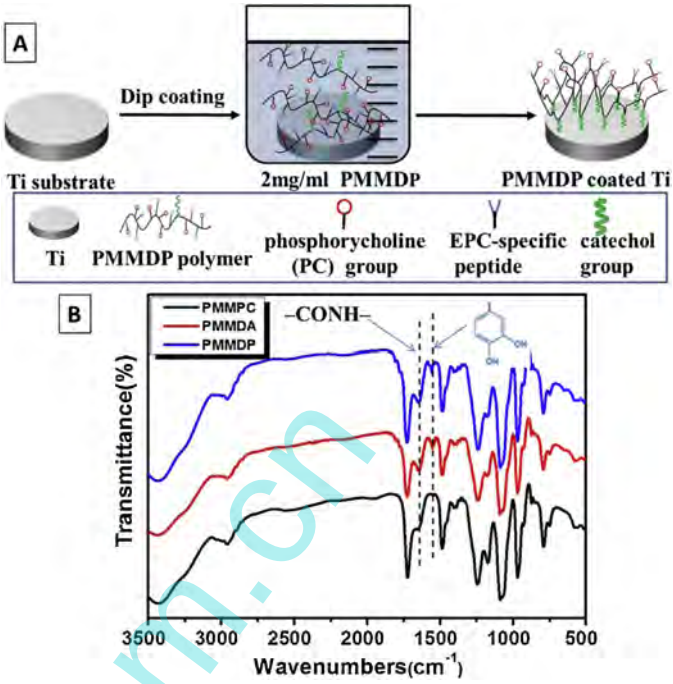

Fig. 2. (A) Sketch map of Ti surface modification procedure using PMMDP; (B) The FTIR spectrum of PMMDP, PMMDA, and PMMPC.

before use, they were dried in an oven for 2 h at 60 °C. Further, the Ti sheets were immersed in an aqueous solution of PMMDP (2.0 mg/ml) at room temperature for 12 h under Ar gas shielding to prepare the multifunctional coatings of Ti-PMMDP. Fig. 2A shows the fabrication process of PMMDP anchored coating on the Ti substrate.

The elemental chemical surface composition was confirmed by X-ray photoelectron spectroscopy (XPS, Kratos Ltd., UK) with a monochromatic Mg Kα excitation radiation ($h\nu$ = 1253.6 eV). Binding energies were calibrated by using the containment carbon (C1s = 284.7 eV). A Shirley background was used, and peaks were fitted using XPSPEAK 4.1 to obtain the high-resolution information.

The amount of PMMDP coated on the titanium surface was quantified using quartz crystal microbalance with dissipation monitoring (QCM-D, Q-Sense, Gothenburg, Sweden) at a fundamental resonant frequency of 5.0 MHz. A 5.0 MHz AT-cut quartz crystal with a gold electrode was used as the working electrode for the QCM experiments. The diameter of the quartz crystal was 13.7 mm and the gold electrode diameter was 5 mm. The Ti-coated (Ti/Au) QCM sensor was obtained from Q-sense (Gothenburg, Sweden).

Initially, the QCM sensor was exposed to phosphate buffer saline (PBS, 0.067 M, pH 7.3) solution at a flow of 50.0 μl/min until a stable baseline of the QCM signals was obtained. The QCM chamber was then filled with 2.0 mg/ml of PMMDP aqueous solution until the frequency was relatively stable. After that, the PBS solution was flowed into the chamber to replace the PMMDP solution and wash away the weakly adsorbed PMMDP from the surface. The adsorbed mass (Δm) was deducted from the frequency shift (Δf) according to the Sauerbrey equation [28]

$$\Delta m = \frac{\Delta f \times C}{n} \quad (1)$$

where C (C = 18.0 ng/cm^2 Hz^{-1} at f_n = 5.0 MHz) is the mass-sensitivity constant and n (n = 1, 3, 5, . . .) is the overtone number.

The surface morphology and roughness of the Ti, Ti-PMMDA and Ti-PMMDP were analyzed by atomic force microscopy (AFM, SPI 3800, NSK Inc.,) in tapping mode. AFM was performed at room

temperature in air at the rate of one line scan per second. Image analysis was performed using the CSPM Imager software.

Static (sessile drop) water contact angles were measured using a goniometer with computer-assisted image analysis (JY-82, China). A droplet of dH_2O was placed on the surface of the sample, and the contact angle was determined using a horizontal microscope. For each sample, the mean value of the contact angle was calculated from at least three individual measurements taken at different locations on the examined samples.

2.5. Stability of the PMMDP coating

The coated PMMDP samples were immersed in PBS (0.067 M, pH 7.3) solution at 37 °C for 22 days (Ti-PMMDP-PBS-22days). Before use, all the soaked samples were taken out of the solution and dried. Further, the surface morphology of the PMMDP coating was observed by scanning electron microscopy (SEM, QUANTA 200, FEI, Netherlands), XPS, and the soaking solution was analyzed by UV spectroscopy.

2.6. Interactions between blood components and substrates

Fresh human blood was obtained from the Blood Central of Chengdu, China, according to the ethical standards in place. The analysis was performed within 12 h after the blood donation. Four parallel samples were used.

2.6.1. Platelet adhesion and Lactate dehydrogenase (LDH) assay

Fresh human citrate-blood was added into centrifuge tubes and subsequently centrifuged at l500 rpm for 15 min to obtain the top layer of PRP. A volume of 60 μl of PRP was distributed on each surface of Ti, and the samples in 24-well plates were incubated for 1 h at 37 °C. Further, the samples were carefully rinsed in 0.9% NaCl solution to remove non-firmly adherent platelets. After fixation with 2.5 wt.% glutaraldehyde solution for 12 h, the samples were dehydrated in graded alcohol solutions (50%, 75%, 90%, 100%; $V_{alcohol}/V_{demineralized\ water}$) and dealcoholized in graded isoamyl acetate solutions (50%, 75%, 90%, 100%; $V_{isoamyl\ acetate}/V_{alcohol}$); all the samples were critical point dried (CPD030, BALZERS) and inspected with an optical microscope (Leica, Germany) or gold sputtered prior to scanning electron microscopy analysis (SEM, Quanta 200, FEI, Holland) to evaluate the morphology and quantity of adherent platelets.

LDH assay was used to detect the amount of adherent platelets. Briefly, 50 μl PRP was added to samples surface and incubated for 1 h at 37 °C. After rinsing with PBS, 40 μl 1% triton solution (Triton X-100 Sigma) was added to each sample and incubated for 5 min at 37 °C. Subsequently, 25 μl lysate was transferred from the surfaces into a 96-well plate and 200 μl chromogenic agent (10 mg/ml Pyr and 10 mg/ml NADH powder dissolved in Tris base buffer) was added before test. The absorbance of different samples was recorded in a microplate reader at 340 nm wavelength. And the amount of adherent platelets was calculated according to the calibration curve.

2.6.2. Platelet activation and p-selectin assay

P-selectin expression was determined as marker of platelet activation induced by the surfaces. Firstly, 50 μl PRP was added to the sample surfaces and incubated for 1 h at 37 °C. Then the samples were rinsed three times with PBS, and used for p-selectin immunofluorescence staining. The above samples were fixed in 4% paraformaldehyde for 12 h at room temperature and rinsed three times with PBS for 3 min each, the samples were then incubated in goat serum (1:10 in PBS) for 1 h at 37 °C to block nonspecific adsorption. Subsequently 30 μl mouse monoclonal anti-human p-selectin antibody (first antibody, 1:200 in PBS) was added to surfaces for 1 h at 37 °C and washed three times with PBS for 3 min each, after that 30 μl FITC-conjugated goat anti-mouse IgG antibody (second antibody, 1:100 in PBS) was added to surfaces and incubated for 30 min at 37 °C and washed three times with PBS for 3 min each. Finally, the samples were observed by fluorescence microscopy (Olympus IX51, Japan).

2.6.3. Fibrinogen denaturation test

For the fibrinogen denaturation test, fresh human blood anticoagulated with citrate was centrifuged at 3000 rpm for 15 min to obtain platelet poor plasma (PPP). Samples were incubated with 60 μl of PPP at 37 °C for 2 h and washed with PBS (5 min × 3 times). Further, the samples were blocked with sheep serum (1/100 dilution in PBS) for 30 min, washed three times with PBS and incubated with 20 μl mouse anti human γ-fibrinogen monoclonal antibody (1:100 dilution, primary antibody, product No: NYB4-2xl-f, Accurate Chemical & Scientific Corp) for 1 h at 37 °C. Subsequently, the samples were once more rinsed with PBS and incubated with horseradish peroxidase labeled goat anti-mouse antibody (1/100 dilution in PBS) for 1 h. Finally, the chromogenic substrate 3,3,5,5-tetramethylbenzidine (TMB) was added and the reaction was stopped using sulfuric acid after 10 min. The absorbance was measured at 450 nm.

2.7. In vitro EPCs culture

Cells were isolated from bone marrow of Sprague-Dawley (SD) rats (Sichuan University, Chengdu, China) [29] and cultured in single-use culture flasks with α-Modified Eagles Eagle's Medium (α-MEM) containing 20% fetal bovine serum (FBS) at 37 °C in a humidified atmosphere with 5% CO_2 [30]. The medium was replaced every 2 days. When the cells were close to confluency, they were trypsinized and cultured in α-MEM supplemented with 20% FBS and 20 ng/ml VEGF. Adherent cells at passage 2 were classified as EPCs according to their morphology and positive expression of markers CD34 and VEGF receptor-2 (VEGFR-2) by using immunofluorescence.

EPCs were then seeded on the samples in a 24-well plate at 5×10^4 cells/ml, and incubated at 37 °C under 5% CO_2. To evaluate the cell affinity of the PMMDP coating (Ti-PMMDP) and the samples after immersion in PBS for 22 days (Ti-PMMDP-PBS-22days), bare Ti and Ti-PMMDA samples were chosen as controls. All samples were sterilized under ultraviolet radiation (27 W, wavelength 254 nm) for 30 min.

After culturing for 1, 3 and 5 days, the adherent cells were fixed on the samples using 2.5% glutaraldehyde solution at 4 °C for 6 h and rinsed with PBS. After that, cells were stained with 4′, 6-diamidino-2-phenylindole (DAPI) and 2-(6-amino-3-imino-3H-xanthen-9-yl) benzoic acid methyl ester (rhodamine) (50 μl per sample) and kept for 30 min in the dark. Fluorescent images were acquired by fluorescent microscope (Olympus IX51, Japan)

EPCs proliferation was investigated by CCK-8 assay after 1, 3 and 5 days of incubation, respectively. The medium was removed and the samples were washed three times with PBS. Subsequently, fresh medium containing CCK-8 reagent was added to each sample and incubated at 37 °C for 3 h in standard culture conditions. The absorbance was measured at 450 nm by a microplate reader. All proliferation experiments were performed in quadruple.

2.8. Data analysis

The data were analyzed using the software SPSS11.5 (Chicago, Illinois, USA). Statistical evaluation of the data was performed using Student's paired test. The probability (p) values $p < 0.05$ were considered to be statistically significant. The results were expressed

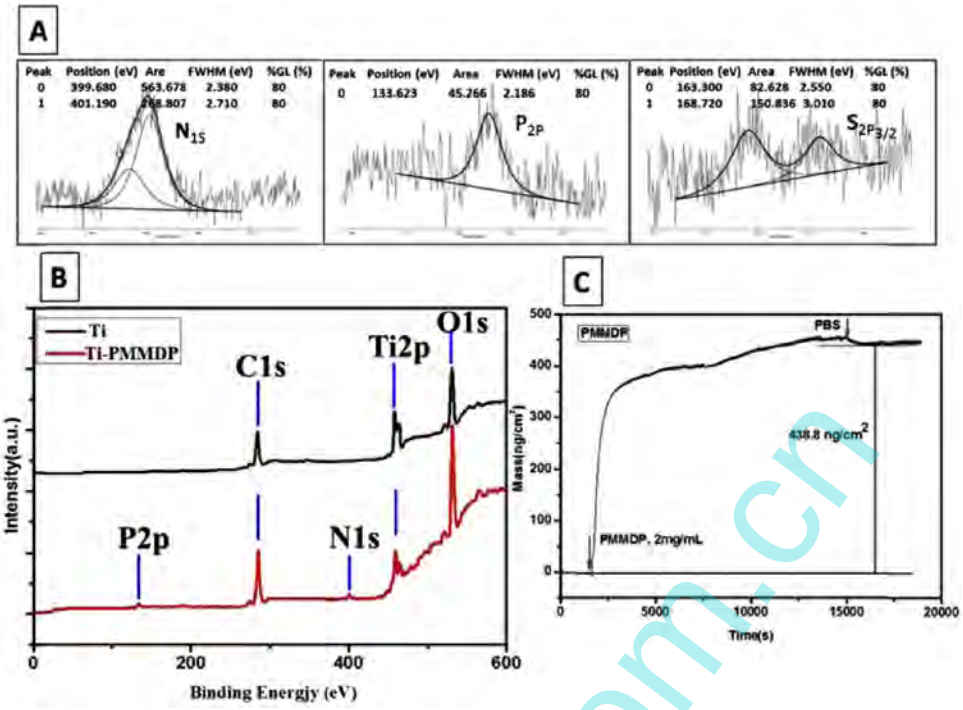

Fig. 3. (A) Element high resolution of XPS analysis of Ti-PMMDP sample surface; (B) XPS full spectrum of Ti and Ti-PMMDP sample surfaces; (C) Mass vs. time curve of PMMDP adsorption determined by QCM measurement.

as mean ± standard deviation (SD). All experiments were repeated three times.

3. Results and discussion

3.1. FTIR characterization of PMMDP co-polymer

FTIR analysis was used to characterize the chemical structure of the PMMDP co-polymer. As shown in Fig. 2B, the basic chemical structures of PMMPC were well maintained in the PMMDA and PMMDP polymers such as the peaks at 1720 cm^{-1} (–COOR, –C=O), 1235 cm^{-1} (–$POCH_2$–), 1086 cm^{-1} (–$OPOCH_2$–), 1173 cm^{-1} (P=O), 969 cm^{-1} (–$N^+(CH_3)_3$), 2958, 1486, 720–790 cm^{-1} (–CH_2–). Compared with PMMPC, the dopamine modified PMMDA showed new peaks at 1553 cm^{-1} (the aromatic ring) and 1639 cm^{-1} (–CONH–). This result confirms the reaction between PMMPC and dopamine and the successful preparation of PMMDA. Additionally, the intensity of the peak at 1639 cm^{-1} (–CONH–) on the spectrum of PMMDP was enhanced, which suggests the introduction of a peptide.

3.2. XPS characterization of PMMDP coating

The surface chemical compositions of the original and modified Ti surfaces were confirmed by XPS analysis. The XPS wide-scan spectra of the samples and their corresponding surface elemental compositions are shown in Fig. 3B. Carbon was present due to unavoidable hydrocarbon contamination, and it was used as an internal reference at 284.6 eV for calibrating peak positions. Different from the bare Ti surface, the new elements phosphorus (P) and nitrogen (N) were introduced by the Ti-PMMDP coating. In the XPS full spectrum of Ti-PMMDP surface, the peak of sulphur (S) element was too weak to be detected.

Fig. 3A shows the high-resolution XPS spectra of the N, P, and S of the Ti-PMMDP surface. Yao et al. [31] reported that the peak of 133.6 eV represents the binding energy of P_{2P} and it was attributed to –$OPOCH_2$– of MPC. Luo et al. [32] revealed that N_{1S} core-level spectra were distributed into two peaks at 399.6 and 401.1 eV. The peak of 401.1 eV was assigned to the –$N^+(CH_3)_3$ group of MPC, and the peak of 399.6 eV was ascribed to –CO–NH–(C,H) and –NH_2 of dopamine and peptide. These were attributed to the introduction of dopamine and peptide based on the condensation reactions. Furthermore, Fang et al. [33] demonstrated that the peaks of 163.3 eV and 168.7 eV represent the binding energy of $S_{2P3/2}$, the peak of 163.3 eV was attributed to the –SH group of peptide, and the peak of 168.7 eV was introduced by the sulfate contaminations during the washing of samples. XPS analysis confirms that the PMMDP coating was successfully constructed on the titanium surface.

3.3. Quantitative analysis of the PMMDP coating

QCM-D is frequently used to investigate the multilayer fabrication and the physical properties of multilayer films. In this study, the adsorption of PMMDP on the substrate was monitored by QCM-D. Fig. 3C presents the curve of mass shift vs. time. The mass of the coating sharply increased in the early stage. For approximately 15,000 s after the reaction, PBS was injected to remove the weakly adsorbed PMMDP. Finally, 438.8 ng/cm^2 of PMMDP was conjugated onto the surface of the QCM sensor coated with Ti. The result confirms the successful immobilization of PMMDP to the substrate. The anchorage of PMMDP to the Ti substrate is believed to be attributed to the chemical bond between the catechol groups of PMMDP and TiO_2, which was spontaneously formed on the surface of the Ti substrate [31].

3.4. Surface morphology and wettability of PMMDP coating

The morphology of the surface observed by AFM is shown in Fig. 4A. The surface of the pristine Ti was smooth with an average roughness of 1.2 nm, rougher (2.1 nm) surface was Ti-PMMDA,

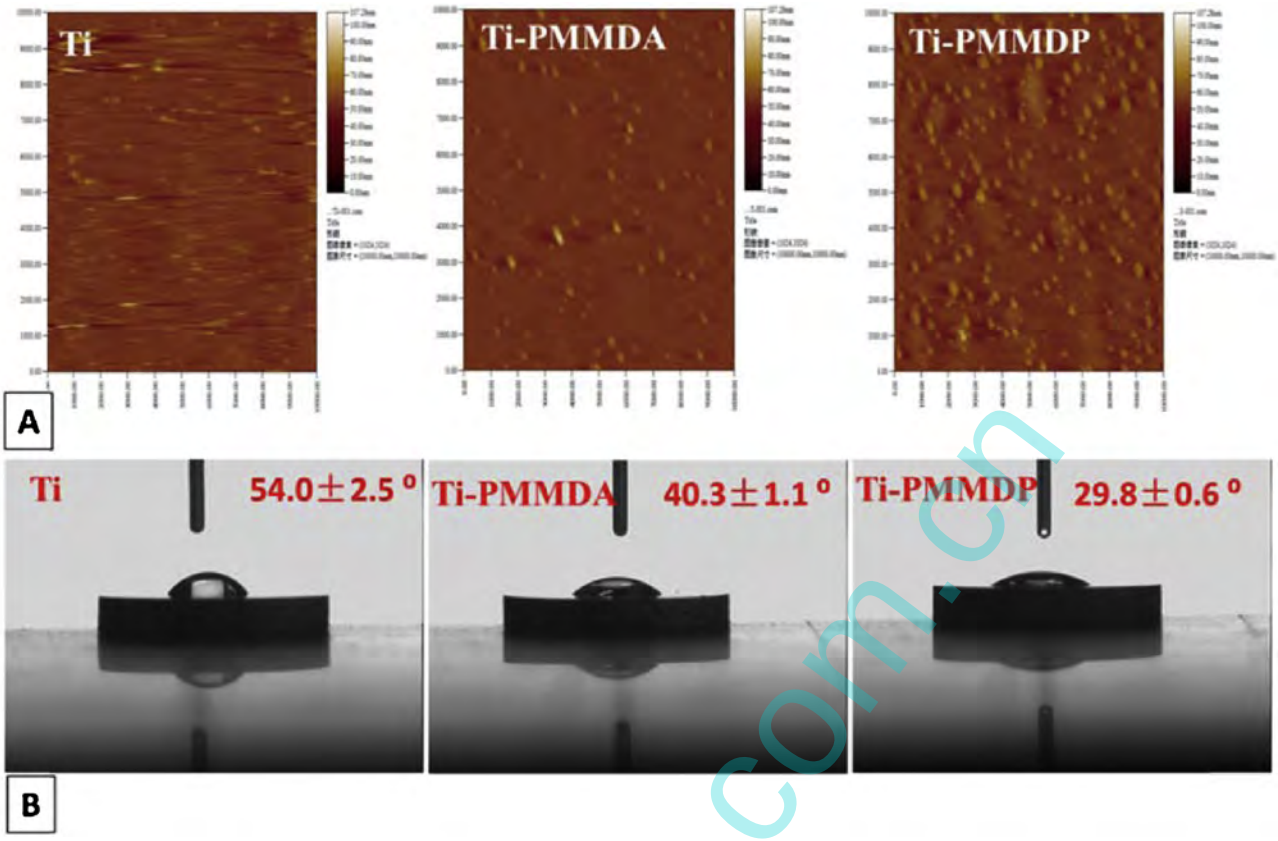

Fig. 4. (A) AFM images of Ti, Ti-PMMDA and Ti-PMMDP sample surfaces; (B) Water contact angle of Ti, Ti-PMMDA and Ti-PMMDP sample surfaces.

and the surface modified with PMMDP became much rougher with a relatively uniform roughness of 3.6 nm. For the implants that come in contact with the blood, such as artificial heart valves and cardiovascular stents, a smooth surface is necessary, with roughness values at the level of protein adsorption (<50 nm), otherwise platelets adhesion and thrombosis occurrence may be more obvious [1]. The slight increase in surface roughness caused by the introduction of PMMDP is well in the acceptable range.

Changes in surface hydrophilicity may cause quantitative and qualitative variations in absorbed proteins, which directly influence the biocompatibility of the materials [34]. Water contact angle was measured to evaluate surface hydrophilicity before and after PMMDP immobilization. As shown in Fig. 4B, the mean water contact angle of Ti ($54.0 \pm 2.4^{\circ}$) decreased dramatically to $29.8 \pm 0.5^{\circ}$ after coating with PMMDP. The increase in surface hydrophilicity can be explained by the exposure of hydrophilic groups such as the phosphorylcholine groups of the PMMDP coating. Hence, hydrophilicity significantly increased after PMMDP immobilization.

3.5. Analysis of the PMMDP coating stability

Fig. 5 shows the stability analysis of the PMMDP coating. It can be observed from the SEM images (Fig. 5A) that the PMMDP coating was homogeneous before immersion. Moreover, several nano-particles can be observed on the image, which may have been formed by the aggregation of the PMMDP polymer molecules, and whose sizes were correlated to the amounts of polymer used. However, no significant change was detected in the morphology of the PMMDP coating after immersion in PBS for 22 days (Ti-PMMDP-PBS-22days), suggesting that the coating exhibits good stability. Meanwhile, the surface element content of Ti-PMMDP and Ti-PMMDP-PBS-22days was analyzed using XPS (Fig. 5B). Results showed a decrease in the N content on the PMMDP coating, from 2.2% (before immersion) to 1.9% (after immersion), showing no significant difference. In addition, the soaking solution of the PMMDP coating was investigated using an UV spectroscopy method (Fig. 5C). There was no significant absorption peak of dopamine observed, proving that no PMMDP polymer was present in the soaking solution. All the results presented above indicated that the PMMDP coating on the Ti surface exhibited good stability.

3.6. Interactions between blood components and substrates

3.6.1. Platelet adhesion and activation

The amount and the activation profile of adherent platelets are considered key indicators for the hemocompatibility evaluation of a material surface. It is generally accepted that platelet morphology is related to its activation level. In this direction the typical shape of round, dendritic, spreading dendritic, spreading and fully spreading corresponds to an activation stage of minor to major [35]. LDH assay was performed for semiquantitative evaluation of the number of adherent platelets. P-selectin assay was performed to further evaluate the platelet activation.

SEM images of adherent platelets on the sample surfaces after 1 h incubation are shown in Fig. 6A. There was a large number of adherent and aggregated platelets on the Ti and Ti-PMMDA sample surfaces, and the adherent platelets mainly exhibited spreading dendritic and fully spreading shape, indicating a significant activation level and poor hemocompatibility. In contrast, the number of platelets on the coated PMMDP surface significantly decreased (Fig. 6A), and the adherent platelets displayed a round shape, which indicated minor activation level and excellent anticoagulant property. In agreement with the SEM result, LDH results showed

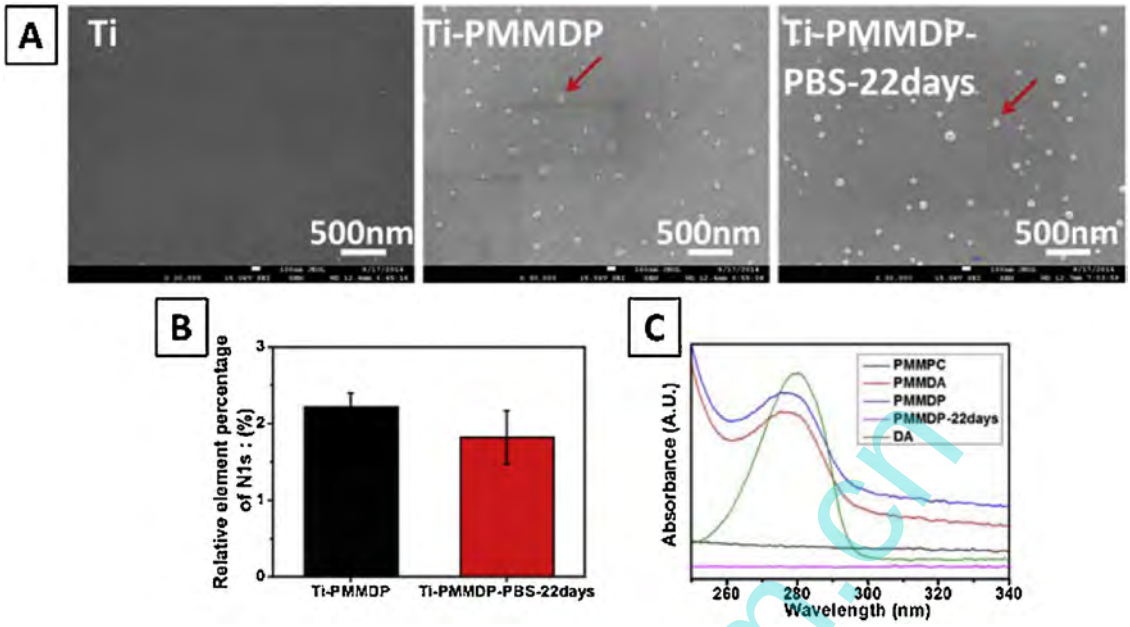

Fig. 5. Characterization of the coating stability (A) SEM images of PMMDP coating before and after immersion in PBS solutions for 22 days; (B) relative elemental percentge of N1s determined by XPS analysis; (C) UV absorption of the soaking solution.

that the platelet number on Ti and Ti-PMMDA sample surfaces was significantly higher ($^*p < 0.05$) than on the Ti-PMMDP surface (Fig. 6B). Fig. 6C shows the p-selectin immunofluorescence staining of adherent platelets on different sample surfaces. Compared with Ti and Ti-PMMDA, the expression of p-selectin on the Ti-PMMDP surface was obviously decreased. The results of SEM, LDH and the p-selectin expression level further proved that the Ti-PMMDP surface could effectively inhibit platelet adhesion and activation.

3.6.2. Fibrinogen denaturation

The conformational change of fibrinogen, i.e., exposure of γ chain (HHLGGAKQAGDV at γ 400–401) [36], plays a critical role in platelet activation and aggregation. Resting platelets interact with adsorbed and denatured, but not with soluble fibrinogen. Fibrinogen is folded in the plasma and little γ chain is exposed, but unfolded or conformational changed when adsorbed on foreign surfaces and the γ chain is exposed. The exposure of the protected γ chain sequences allow fibrinogen to bind to the GPIIb/IIIa integrin receptor on platelet membrane and further cause the adhesion and aggregation of platelets [37]. Therefore, conformational changes of fibrinogen, measured by immunochemistry, reveal the thrombosis tendency. Fig. 6D displays the fibrinogen denaturation on different surfaces. The PMMDP-coated samples showed significantly smaller absorbance values compared to Ti and Ti-PMMDA samples. This result demonstrates that the Ti-PMMDP surface decreases the denaturation of fibrinogen.

3.7. EPCs adhesion and proliferation

The morphology and the density of attached EPCs were presented in Fig. 7A. The EPCs on Ti-PMMDP and Ti-PMMDP-PBS-22days surface were fusiform after 1 day in culture, followed by a rapid proliferation, as seen on day 3rd and 5th. On the Ti and Ti-PMMDA sample surfaces, there were less adherent EPCs, some of them were round and did not spread. This difference is consistent with the result of the CCK-8 assay.

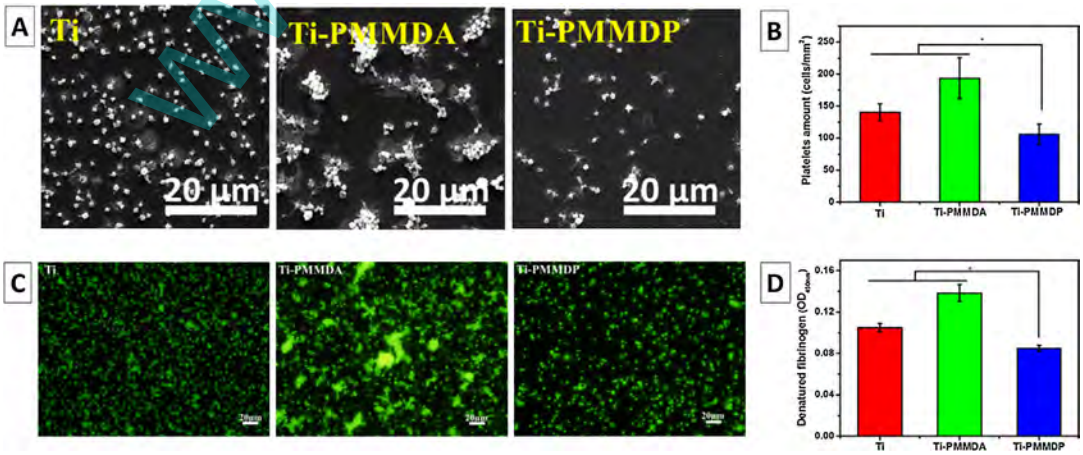

Fig. 6. (A) SEM images of platelets on the sample surfaces after incubation with PRP for 1 h; (B) amount of adherent platelets on various sample surfaces measured by LDH assay after incubation with PRP for 1 h; (C) P-selectin immunofluorescence staining of activated platelets on different sample surfaces; (D) Denatured fibrinogen on the surface evidenced by immunochemistry ($^*p < 0.05$, mean ± SD, $N = 4$).

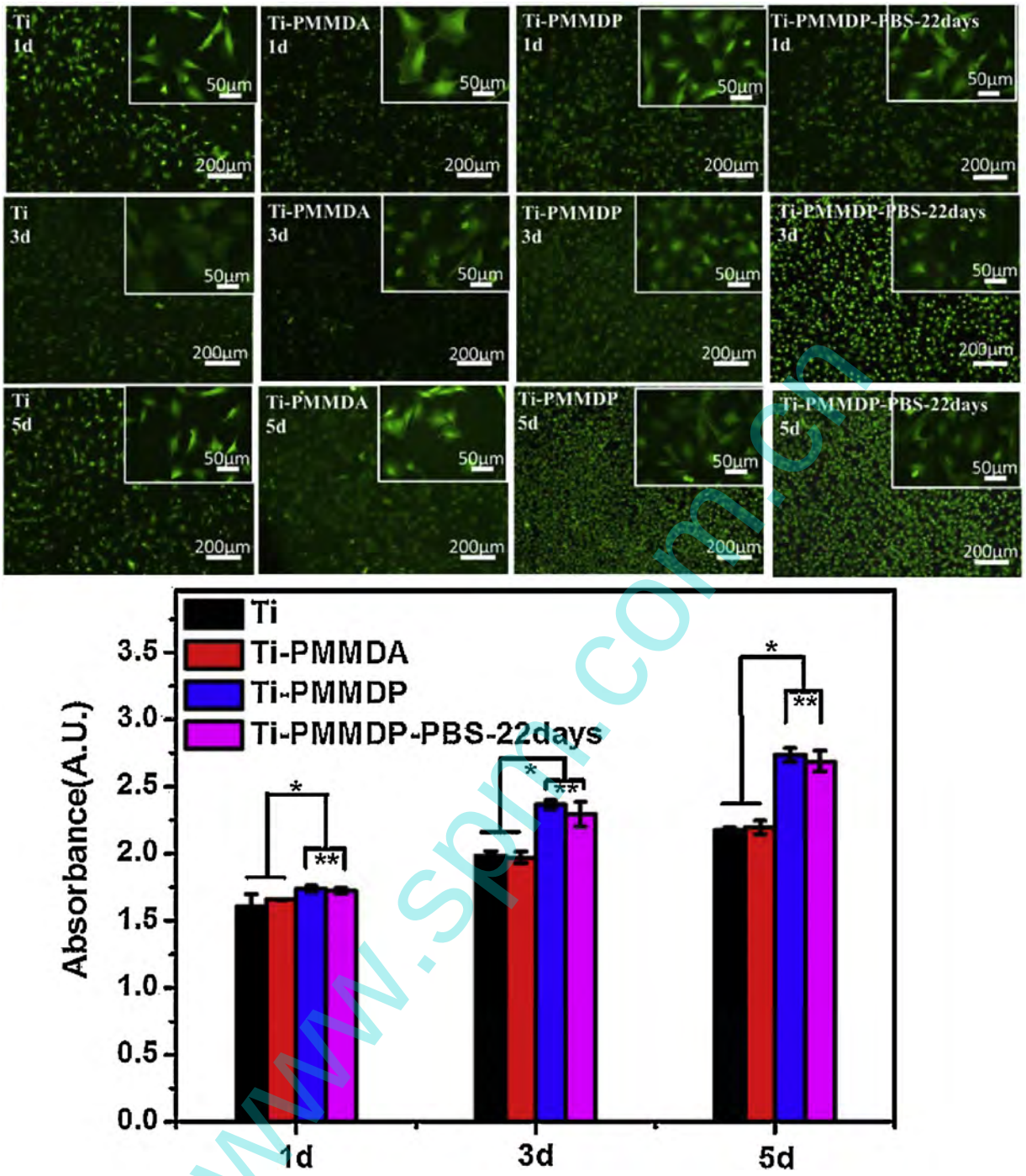

Fig. 7. (A) Fluorescence micrographs of rhodamine123 stained EPCs after culture on the surfaces of Ti, Ti-PMMDA, Ti-PMMDP and Ti-PMMDP-PBS-22days samples for 1, 3 and 5 days; (B) EPCs attachment and proliferation on Ti, Ti-PMMDA, Ti-PMMDP and Ti-PMMDP-PBS-22days surfaces determined using the metabolic CCK-8 assay ($^{*}p < 0.05$, $^{**}p > 0.05$, mean ± SD, $N = 4$).

The effect of PMMDP coating on EPCs attachment and proliferation was investigated by a CCK-8 viability assay after incubation for 1, 3 and 5 days, respectively. Fig. 7B shows the number of EPCs and their proliferation rate on the bare Ti, Ti-PMMDA, Ti-PMMDP and Ti-PMMDP-PBS-22days surfaces. The conversion of CCK-8 to the colored product was measured proportional to the number of cells. After 1, 3 and 5 days in culture, the EPCs on the Ti-PMMDP and Ti-PMMDP-PBS-22days surfaces exhibited distinctly enhanced attachment and proliferation compared with those on the control Ti and Ti-PMMDA ($p < 0.05$), but there was no significant difference between Ti-PMMDP and Ti-PMMDP-PBS-22days surfaces. The results demonstrated that the EPCs-specific peptide of the PMMDP coating supported EPCs attachment and proliferation even after immersion in PBS for 22 days. Apparently, the biofunctional coating improves the adhesion and proliferation of EPCs.

4. Conclusions

A novel polymer (PMMDP), bearing phospholipid groups and EPCs-specific peptides, was synthesized by a facile method. A stable coating of PMMDP was constructed on Ti only by immersion into an aqueous PMMDP solution at room temperature. The PMMDP

coating has great potential for application in blood-contacting materials to realize rapid endothelialization through capturing circulating EPCs.

Acknowledgements

This work was financially supported by the National Physiological Science Foundation of China (nos. 30870629, 50971107), Key Basic Research Project (no. 2011CB606204), Sci-technical Support Project of Sichuan Province (2013SZ0077), Fundamental Research Funds for the Central Universities (no. SWJTU11ZT11) and Foundation of Jiangsu Provincial Key Laboratory for Interventional Medical Devices (JR1205).

References

[1] G.C. Li, P. Yang, W. Qin, M.F. Maitz, S. Zhou, N. Huang, The effect of coimmobilizing heparin and fibronectin on titanium on hemocompatibility and endothelialization, Biomaterials 32 (2011) 4691–4703.
[2] D.F. Williams, On the mechanisms of biocompatibility, Biomaterials 29 (2008) 2941–2953.
[3] A. Andukuri, M. Kushwaha, A. Tambralli, J.M. Anderson, D.R. Dean, J.L. Berry, Y.D. Sohn, Y.S. Yoon, B.C. Brott, H.W. Jun, A hybrid biomimetic nanomatrix composed of electrospun polycaprolactone and bioactive peptide amphiphiles forardiovascular implants, Acta Biomater. 7 (2011) 225–233.
[4] Q. Li, Z.H. Wang, S. Zhang, W.T. Zheng, Q. Zhao, J. Zhang, L.Y. Wang, S.F. Wang, D.L. Kong, Functionalizatin of the surface of electrospun poly(epsilon-caprolactone) mats using zwitterionic poly(carboxybetaine methacrylate) and cell-specific peptide for endothelial progenitor cells capture, Mater. Sci. Eng. C: Mater. 33 (2013) 1646–1653.
[5] R.E. Unger, K. Peters, M. Wolf, A. Mottab, C. Migliaresi, C.J. Kirkpatrick, Endothelialization of a non-woven silk fibroin net for use in tissue engineering: growth and gene regulation of human endothelial cells, Biomaterials 25 (2004) 5137–5146.
[6] A. Lichtenberg, I. Tudorache, S. Cebotari, S.R. Lichtenberg, G. Sturz, K. Hoeffler, C. Hurscheler, G. Brandes, A. Hilfiker, A. Haverich, In vitro re-endothelialization of detergent decellularized heart valves under simulated physiological dynamic conditions, Biomaterials 27 (2006) 4221–4229.
[7] T. Asahara, T. Murohara, A. Sullivan, M. Silver, R. van der Zee, T. Li, B. Witzenbichler, G. Schatteman, J.M. Isner, Isolation of putative progenitor endothelial cells for angiogenesis, Science 275 (1997) 964–967.
[8] A. Andukuri, Y.D. Sohn, C.P. Anakwenze, D.J. Lim, B.C. Brott, Y.S. Yoon, H.W. Jun, Enhanced human endothelial progenitor cell adhesion and differentiation by a bioinspired multifunctional nanomatrix, Tissue Eng. Part C 5 (2013) 375–385.
[9] M. Avci-Adali, A. Paul, G. Ziemer, H.P. Wendel, New strategies for in vivo tissue engineering by mimicry of homing factors for self-endothelialisation of blood contacting materials, Biomaterials 29 (2008) 3936–3945.
[10] T. Takahashi, C. Kalka, H. Masuda, D. Chen, M. Silver, M. Kearney, M. Magner, J.M. Isner, T. Asahara, Ischenia- and cytokine-induced mobilization of bone marrow-dervied endothelial progenitor cells for neovascularization, Nat. Med. 5 (1999) 434–438.
[11] J. Aoki, P.W. Serruy, H. van Beusekom, A.T. Ong, E.P. McFadden, G. Sianos, W.J. van der Giessen, E. Regar, P.J. de Feyter, H.R. Davis, S. Rowland, M.J.B. Kutryk, Endothelial progenitor cell capture by stents coated with antibody against CD34: the HEALING-FIM (Healthy Endothelial Accelerated Lining Inhibits Neointimal Growth-First In Man) Registry, J. Am. Coll. Cardiol. 45 (2005) 1574–1579.
[12] M.W. Vaughn, L. Kuo, J.C. Liao, Effective diffusion distance of nitric oxide in the microcirculation, Am. J. Physiol. 274 (1998) H1705–H1714.
[13] A.N. Veleva, D.E. Heath, S.L. Cooper, C. Patterson, Selective endothelial cell attachment to peptide-modified terpolymers, Biomaterials 29 (2008) 3656–3661.
[14] R. Blindt, F. Vogt, I. Astafieva, C. Fach, M. Hristov, N. Krott, B. Seitz, A. Kapurniotu, C. Kwok, M. Dewor, A.K. Bosserhoff, J. Bernhagen, P. Hanrath, R. Hoffmann, C. Weber, A novel drug-eluting stent coated with an integrinbinding cyclic Arg-Gly-Asp peptide inhibits neointimal hyperplasia by recruiting endothelial progenitor cells, J. Am. Coll. Cardiol. 47 (2006) 1786.
[15] L. Biancone, V. Cantaluppi, D. Duo, M.C. Deregibus, C. Torre, G. Camussi, Role of L-selectin in the vascular homing of peripheral blood-derived endothelial progenitor cells, J. Immunol. 173 (2004) 5268–5274.
[16] E.J. Suuronen, P. Zhang, D. Kuraitis, X. Cao, A. Melhuish, D. McKee, F. Li, T.G. Mesana, J.P. Veinot, M. Ruel, An acellular matrix-bound ligand enhances the mobilization, recruitment and therapeutic effects of circulating progenitor cells in a hindlimb ischemia model, FASEB J. 23 (2009) 1447–1458.
[17] J. Hoffmann, A. Paul, M. Harwardt, J. Groll, T. Reeswinkel, D. Klee, M. Moeller, H. Fischer, T. Walker, T. Greiner, G. Ziemer, H.P. Wendel, Immobilized DNA aptamers used as potent attractors for porcine endothelial precursor cells, J. Biomed. Mater. Res. A 84 (2008) 614–621.
[18] J. Hur, C.H. Yoon, H.S. Kim, J.H. Choi, H.J. Kang, K.K. Hwang, B.H. Oh, M.M. Lee, Y.B. Park, Characterization of two types of endothelial progenitor cells and their different contributions to neovasculogenesis, Arterioscler. Thromb. Vasc. Biol. 24 (2004) 288–293.
[19] E. Rohde, C. Malischnik, D. Thaler, T. Maierhofer, W. Linkesch, G. Lanzer, C. Guelly, D. Strunk, Blood monocytes mimic endothelial progenitor cells, Stem Cells 24 (2006) 357–367.
[20] M.C. Yoder, L.E. Mead, D. Prater, T.R. Krier, K.N. Mroueh, F. Li, R. Krasich, C.J. Temm, J.T. Prchal, D.A. Ingram, Redefining endothelial progenitor cells via clonal analysis and hematopoietic stem/progenitor cell principals, Blood 109 (2007) 1801–1809.
[21] D.A. Ingram, L.E. Mead, H. Tanaka, V. Meade, A. Fenoglio, K. Mortell, K. Pollok, M.J. Ferkowicz, D. Gilley, M.C. Yoder, Identification of a novel hierarchy of endothelial progenitor cells using human peripheral and umbilical cord blood, Blood 104 (2004) 2752–2760.
[22] Y. Iwasaki, K. Ishihara, Phosphorylcholine-containing polymers for biomedical applications, Anal. Bioanal. Chem. 381 (2005) 534–546.
[23] Y.C. Zhao, Q.F. Tu, J. Wang, Q.J. Huang, N. Huang, Crystalline TiO_2 grafted with poly(2-methacryloyloxyethyl phosphorylcholine) via surface-initiated atom-transfer radical polymerization, Appl. Sci. 257 (2010) 1596–1601.
[24] H. Lee, S.M. Dellatore, W.M. Miller, P.B. Messersmith, Mussel-inspired surface chemistry for multifunctional coatings, Science 318 (2007) 426–430.
[25] H. Lee, N.F. Scherer, P.B. Messersmith, Single-molecule mechanics of mussel adhesion, Proc. Natl. Am. Sci. U.S.A. 103 (2006) 12999–13993.
[26] Y. Ji, Y. Wei, X. Liu, J. Wang, K. Ren, J. Ji, Zwitterionic polycarboxybetaine coating functionalized with REDV peptide to improve selectivity for endothelial cells, J. Biomed. Mater. Res. A 100 (2012) 1387–1397.
[27] B. Byambaa, T. Konno, K. Ishihara, Detachment of cells adhered on the photoreactive phospholipid polymer surface by photoirradiation and their functionality, Colloids Surf. B: Biointerfaces 103 (2013) 489–495.
[28] G. Sauerbrey, Verwendung von Schwingquarzen zur Wägung dünner Schichten und zur Mikrowägung, Z. Physik 155 (1959) 206–222.
[29] C. Chen, J.Y. Chen, Q.L. Li, Q.F. Tu, S.M. Chen, S.H. Liu, N. Huang, The biological behavior of endothelial progenitor cells on titanium surface immobilized by anti-CD34 antibody, Adv. Mater. Res. 79–82 (2009) 707–710.
[30] Q.L. Li, N. Huang, C. Chen, J.L. Chen, K.Q. Xiong, J.Y. Chen, T.X. You, J. Jin, X. Liang, Oriented immobilization of anti-CD34 antibody on titanium surface for self-endothelialization induction, J. Biomed. Mater. Res. A 94 (2010) 1283–1293.
[31] Y. Yao, K. Fukazawa, N. Huang, K. Ishihara, Effects of 3, 4-dihydrophenyl groups in water-soluble phospholipid polymer on stable surface modification of titanium alloy, Colloids Surf. B: Biointerfaces 88 (2011) 215–220.
[32] R.F. Luo, L.L. Tang, J. Wang, Y.C. Zhao, Q.F. Tu, Y.J. Weng, R. Shen, N. Huang, Improved immobilization of biomolecules to quinone-rich polydopamine for efficient surface functionalization, Colloids Surf. B: Biointerfaces 106 (2013) 66–73.
[33] Z. Fang, Y.F. Liu, Y.T. Fan, Y.H. Ni, X.W. Wei, K.B. Tang, J.M. Shen, Y. Chen, Epitaxial growth of CdS nanoparticle on Bi_2S_3 nanowire and photocatalytic application of the heterostructure, J. Phys. Chem. C 115 (2011) 13968–13976.
[34] E. Monchaux, P. Vermete, Effects of surface properties and bioactivation of biomaterials on endothelial cells, Front. Biosci. (Schol. Ed.) 2 (2010) 239–2255.
[35] Y.J. Weng, Q. Song, Y.J. Zhou, L.P. Zhang, J. Wang, J.Y. Chen, Y.X. Leng, S.Y. Li, N. Huang, ImmoBiomatbilization of selenocystamine on TiO_2 surface for in situ catalytic generation of nitric oxide and potential application in intravascular stents, Biomaterials 32 (2011) 1253–1263.
[36] M. Kloczewiak, S. Timmons, T.J. Lukas, J. Hawiger, Platelet receptor recognition site on human-fibrinogen-synthesis and structure-function relationship of peptides corresponding to the carboxy-terminal segment of the gamma chain, Biochem. J. 23 (1984) 1767–1774.
[37] J.N. Baumgartner, S.L. Cooper, Influence of thrombus components in mediating *Staphylococcus aureus* adhesion to polyurethane surfaces, J. Biomed. Mater Res. 40 (1998) 660–670.